

Research Article: New Research | Sensory and Motor Systems

Active vision in sight recovery individuals with a history of long-lasting congenital blindness

https://doi.org/10.1523/ENEURO.0051-22.2022

Cite as: eNeuro 2022; 10.1523/ENEURO.0051-22.2022

Received: 3 February 2022 Revised: 10 August 2022 Accepted: 17 August 2022

This Early Release article has been peer-reviewed and accepted, but has not been through the composition and copyediting processes. The final version may differ slightly in style or formatting and will contain links to any extended data.

Alerts: Sign up at www.eneuro.org/alerts to receive customized email alerts when the fully formatted version of this article is published.

Copyright © 2022 Ossandón et al.

This is an open-access article distributed under the terms of the Creative Commons Attribution 4.0 International license, which permits unrestricted use, distribution and reproduction in any medium provided that the original work is properly attributed.

- 2 Abbreviated Title: Active vision despite congenital blindness
- 3 José P. Ossandón¹*, Paul Zerr^{1,2}, Idris Shareef³, Ramesh Kekunnaya³, Brigitte Röder¹
- 4 ¹ Biological Psychology and Neuropsychology, Hamburg University, Hamburg, Germany
- 5 ² Experimental Psychology, Helmholtz Institute, Utrecht University, Utrecht, The Netherlands
- 6³ Child Sight Institute, Jasti V Ramanamma Children's Eye Care Center, LV Prasad Eye Institute,
- 7 Hyderabad, India
- 8 Author contributions: J.P.O and B.R. designed the research; R.K. and I.S identified and evaluated the
- 9 clinical population; J.P.O., I.S. and P.Z. performed the research; J.P.O analyzed the data; J.P.O and B.R
- 10 wrote the paper; all authors edited and approved the manuscript.
- 11 Correspondence should be addressed to José P. Ossandón, jose.ossandon@uni-hamburg.de
- 12
- 13 Number of Figures: 4 Number of Tables: 1
- 14 Number of Multimedia: 1 Number of words for Abstract: 182
- 15 Number of words for Significance Statement: 118
- 16 Number of words for Introduction: 747
- 17 Number of words for Discussion: 1936
- 18
- 19 Acknowledgments: The authors are grateful to D. Balasubramanian who made the research at the LV
- 20 Prasad Eye Institute possible. We thank Kabilan Pitchaimuthu and Prativa Regmi for clinical data curation
- 21 and Suddha Sourav and Rashi Pant for technical support.
- 22 Conflict of Interest: Authors report no conflict of interest.
- Funding sources: This work was supported by the German Research Foundation (DFG) (grants Ro
 2625/10-1 and SFB936 178316478 B11).
- 26

27 Active vision in sight recovery individuals with a history of long-

28 lasting congenital blindness

29

30 ABSTRACT

31 What we see is intimately linked to how we actively and systematically explore the world through 32 eye movements. However, it is unknown to what degree visual experience during early development is necessary for such systematic visual exploration to emerge. The present study 33 investigated visual exploration behavior in ten human participants whose sight had been restored 34 35 only in childhood or adulthood, after a period of congenital blindness due to dense bilateral 36 congenital cataracts. Participants freely explored real-world images while their eye movements were recorded. Despite severe residual visual impairments and gaze instability (nystagmus), 37 38 visual exploration patterns were preserved in individuals with reversed congenital cataract. Modelling analyses indicated that similar to healthy controls, visual exploration in individuals 39 40 with reversed congenital cataract was based on the low-level (luminance contrast) and high-level 41 (object components) visual content of the images. Moreover, participants used visual short-term 42 memory representations for narrowing down the exploration space. More systematic visual 43 exploration in individuals with reversed congenital cataract was associated with better object recognition, suggesting that active vision might be a driving force for visual system development 44 45 and recovery. The present results argue against a sensitive period for the development of neural mechanisms associated with visual exploration. 46

47

48 SIGNIFICANCE STATEMENT

49 Humans explore the visual world with systematic patterns of eye movements, but it is unknown 50 whether early visual experience is necessary for the acquisition of visual exploration. Here, we 51 show that sight recovery individuals who had been born blind demonstrate highly systematic eye 52 movements while exploring real-world images, despite visual impairments and pervasive gaze 53 instability. In fact, their eye movement patterns were predicted by those of normally sighted 54 controls and models calculating eye movements based on low- and high-level visual features, and 55 they moreover took memory information into account. Since object recognition performance was 56 associated with systematic visual exploration it was concluded that eye movements might be a 57 driving factor for the development of the visual system.

58 INTRODUCTION

59 Prolonged visual deprivation from birth has been observed to result in the irreversible impairment 60 of several visual functions (Lewis and Maurer, 2005; Röder and Kekunnaya, 2021a). These 61 findings have been taken as evidence for "sensitive periods" in brain development, defined as 62 epochs during which adequate input is essential for full functional development (Knudsen, 2004; Hensch, 2005). In humans, sensitive periods have been studied in individuals who had been born 63 blind or with severe visual impairments due to dense, bilateral cataracts and who later received 64 cataract-removal surgery at different times during infancy, childhood or even adulthood (Maurer 65 et al., 2007; Röder et al., 2013; Ganesh et al., 2014). Despite improvements in vision after 66 congenital cataract removal (Wright et al., 1992), basic visual abilities such as visual acuity 67 68 (Ellemberg et al., 1999; Lambert et al., 2006) remain permanently impaired, especially if cataracts 69 are not treated within the first few weeks of life. Moreover, higher order visual functions such as 70 feature binding and within-category viewpoint-independent discrimination, particularly of faces, have been found to only partially recover after congenital cataract surgery, and not to the degree 71 expected by the recovery of visual acuity (Le Grand et al., 2001; Putzar et al., 2007, 2010; 72 Ostrovsky et al., 2009). In addition to these perceptual deficits, individuals who had prolonged 73 74 congenital bilateral visual deprivation (>8 weeks) typically also suffer from nystagmus (Rogers et 75 al., 1981; Lambert et al., 2006; Birch et al., 2009). Nystagmus is a disorder of gaze stability that results in continuous, periodic and involuntary motion of the eyes. 76 77 It has recently been shown that despite some distortions due to the superimposed

nystagmus, eye movements to simple visual stimuli were reasonably precise and fast in
individuals with reversed congenital cataract (Zerr et al., 2020). However, it is unclear whether
higher levels of ocular control, such as the ability to generate typical patterns of active visual
exploration of natural stimuli, recover after a transient phase of congenital visual deprivation.
Active visual exploration is crucial for visual functions such as visual search and object

83 identification, especially in noisy or ambiguous conditions (Einhauser et al., 2004; Holm et al., 84 2008; Kietzmann et al., 2011). Furthermore, active visual exploration has been shown to be 85 relevant for visual memory formation in typically sighted individuals (Hannula, 2010). 86 Previous research has suggested that visual exploration is guided by both bottom-up 87 (stimulus-driven) and top-down mechanisms, which jointly define the direction towards which the eves move. Stimulus-driven mechanisms use input characteristics such as luminance, color, 88 89 orientation and motion (Veale et al., 2017); whereas top-down mechanisms consider goals, 90 memory, and contextual factors (Eckstein, 2011; Tatler et al., 2011; König et al., 2016). Stimulus-91 driven "saliency" models have successfully utilized low- and high-level visual features to predict 92 human eye movements during free-viewing of scenes (Itti and Koch, 2000; Tatler et al., 2005; 93 Kümmerer et al., 2017). Additionally, the repeated presentation of the same image has been used 94 to assess the effects of short-term memory on visual exploration, that is, a non-reflexive aspect of 95 gaze control (Ryan et al., 2000; Smith et al., 2006; Kaspar and König, 2011). If an image is repeatedly encountered, the spread of visual exploration decreases (Hannula, 2010). It has been 96 97 hypothesized that short-term memory representations provide top-down information, which, 98 combined with bottom-up stimulus-driven maps in so called priority maps, guide eye movements 99 (Veale et al., 2017). 100 The degree to which the development of bottom-up and top-down mechanisms of active

visual exploration depend on typical visual input after birth is unknown. Theories from
developmental psychology have suggested that active visual exploration in infants is instrumental
for the development of object knowledge (Johnson and Johnson, 2000). It remains to be
investigated whether visual recovery after late sight restoration affects bottom-up, stimulus-driven
visual exploration (Einhäuser et al., 2008a; Açık et al., 2009; Nuthmann and Henderson, 2010),

106 and/or top-down, for instance, memory based visual exploration (Hannula, 2010).

Active vision despite congenital blindness

107 In the present study, we employed a free-viewing task in a sample of 10 individuals who had been born with dense, bilateral cataracts which had been surgically removed later in life (CC 108 109 group, see Table 1) - in some participants, only in late childhood or adulthood. The distribution of gazed locations elicited by photographic stimuli (close-up images of different objects, plants, 110 animals and buildings) were assessed and compared to the typical visual exploration patterns of 111 age-matched, normally sighted controls (SC group). Further, the CC group was compared to 112 113 individuals with nystagmus due to reasons other than congenital cataracts (nystagmus controls, NC group), and individuals with a history of developmental cataracts (developmental cataract 114 115 reversal group, DC group), in order to isolate group differences specific to early visual 116 deprivation rather than a general history of visual deficits. Additionally, we tested how well visual 117 exploration in individuals with reversed congenital cataract was predicted by low- and high-level 118 saliency models. Finally, to explore top-down influences on visual exploration, the effects of 119 short-term memory on eye movements were assessed by assessing the adaptation of visual 120 exploration patterns for images which were repeatedly presented.

Table 1: Participants description

	Age at testing in years	Age at surgery in months	Cataract type at surgery	Presurgical visual acuity (best eye)	Most recent v (CC/DC: post (best eye) Decimal	-	Cataract Family history
Congenital		oup (CC, N =	<u> </u>	(00010)0)	Deennar	10511111	5
cc-1	16.9	4	dense	FFL+	0.33	0.47	no
cc-2	13.5	83	absorbed	CF 3m	0.15	0.79	no
cc-3	31.7	168	absorbed	unknow	0.1	1	yes
cc-4	42.9	264	absorbed	0.06 (decimal)	0.16	0.79	yes
cc-5	16.1	186	absorbed	0.03 (decimal)	0.08	1.1	no
cc-6	12.3	138	dense	CF CF	0.03	1.4	yes
cc-7	21.7	213	dense	CF 0.5m	0.12	0.9	yes
cc-8	10.7	17	dense	PL at 0.5m	0.25	0.6	no
cc-9	23.5	3	dense	FFL-	0.25	0.6	no
cc-10	17.2	34	dense	FFL+	0.16	0.79	no
summary	M:20.7	M:111 (9.2			GM: 0.14	M: 0.86	
•	R:10-42	years)			R: 0.03 – 0.3	R: 0.47 – 1.4	
		R: 4 – 264					

Developmental cataract control group (DC, N = 9)

			P (,				
dc-1	24.4	31	not dense	FFL +	0.5	0.3	no
dc-2	13.8	89	dense	CF 1 m	0.66	0.17	unknown
dc-3	16.2	130	not dense	0.4	0.8	0.09	no
dc-4	13.2	71	dense	FFL +	0.46	0.33	unknown
dc-5	17.3	91	not dense	0.16	0.8	0.09	unknown
dc-6	11.5	91	not dense	0.25	0.8	0.09	unknown
dc-7	18.8	208	not dense	0.2	0.7	0.13	no
dc-8	11.6	54	dense	CF 1 m	1	0	unknown
dc-9	13.5	30	dense	FFL +	0.66	0.17	unknown
summary	M:15.6	M: 88.3 (7.4	4 dense		GM: 0.7	M: 0.16	
	R:11 – 24	years) R: 30 – 208			R: 0.46 – 1	R: 0 – 0.33	

Nystagmus control group (NC, N = 10)

summary	M:15		GM: 0.45	M: 0.35	
	R: 8 – 37		R: 0.25 - 0.8	R: 0.1 – 0.6	

Normally sighted control group (SC, N = 13)

summary	M: 23.7				1 (all)	0 (all)	
-	R: 11 – 40						

PL: perception light; CF: counting finger, equivalence with logMAR acuity has been reported to be 1.7-2.0 at 30 cm (Schulze-Bonsel et al., 2006); CF CF: counting finger close to face; FFL: fixate and follows light; M: mean; GM: geometric mean, R: range.

Extended data Table 1-1 shows the relationship between visual acuity and age of surgery (CC and DC groups) and age of testing (all groups).

121 122

123 MATERIALS AND METHODS

124 Participants

125 A total of 42 participants from four different populations were recruited at the LV Prasad Eye126 Institute and the local community of Hyderabad (India).

(1) Congenital cataract reversal individuals (CC group): Individuals were selected from a large number of patients who had been treated with the diagnosis of congenital cataracts. Based on medical records, a clinical history of bilateral congenital cataracts and a history of patterned visual deprivation were confirmed. A lack of fundus view and a lack of retinal glow were considered as evidence for the absence of patterned input reaching the retina prior to cataract surgery. Additionally, the presence of nystagmus, sensory strabismus, positive family history as well as absorbed lenses aided in the classification of CC participants.

134 The CC group consisted of 10 participants (2 females; mean age: 20.7 years; range: 10.7 – 42.9) who had received cataract removal surgery at a mean age of 9.2 years (range: 3 months - 22 135 years). These individuals were tested on average 11.4 years after cataract removal surgery (range: 136 137 7 months – 23.2 years). Of the 10 participants, 5 had a documented history of strabismus (2 138 esotropia/3 exotropia), 7 had implanted intraocular lenses, and the remaining 3 used corrective 139 glasses. Four CC individuals had a documented family history of congenital cataracts, and 4 CC 140 individuals had absorbed cataracts when presented at the LV Prasad Eye Institute. Absorption of 141 cataracts in middle to late childhood has been regularly observed in individuals born with dense 142 congenital cataracts. Absorbed cataracts can be unambiguously differentiated from non-dense or 143 partial cataracts by, for instance, the morphology of the lens, anterior capsule wrinkling, as well 144 as plaque or thickness of the stroma. Absorbed cataracts strongly imply dense cataracts, and therefore blindness, at birth. Pre-surgical visual acuity measurements in severely visually 145 146 deprived individuals confirmed that at least 7 out of 10 CC individuals were blind (i.e. had a 147 visual acuity of less than 3/60) (World Health Organization, 2019). The remaining three CC

individuals had absorbed lenses; their pre-surgery vison corresponded to severe visual
impairment, as defined by the WHO. All CC participants additionally suffered from nystagmus,
which is strong evidence for the absence of patterned vision at birth. CC participants' postsurgical visual acuity of the better eye ranged from 0.03 to 0.33 decimal units (geometric mean:
0.14; logMar: 0.47 – 1.4, logMar mean: 0.86). A detailed description of CC participants is
presented in Table 1 (and Extended data Table 1-1).

154 (2) Developmental cataract reversal group (DC group): This control group allowed us to estimate the role of vision at birth for the acquisition of visual exploration behavior. The DC 155 group consisted of nine individuals (4 females, mean age: 15.6 years, range: 11.6 - 24.4) with a 156 history of bilateral cataracts, but not dense and/or congenital cataracts. These individuals allowed 157 us to control for task independent effects on eye movements due to cataract surgery (e.g., 158 159 exploring the images with intraocular lenses). Cataract removal surgery had been performed at a mean age of 7.4 years (range: 2.8 - 17.3 years); they were tested on average 8.2 years (range: 1.5160 21.8 years) post-surgery. DC participants' post-surgical visual acuity ranged from 0.46 to 1 161 _ decimal units (geometrical mean: 0.7; logMar: 0 - 0.33, logMar mean: 0.16). All DC participants 162 were fitted with intraocular lenses. 163

Retrospective classification of CC and DC participants comes with some degree of uncertainty. However, the use of the classification criteria as implemented in the present study have recently been confirmed by an electrophysiological biomarker (Sourav et al., 2020).

(3) Nystagmus group (NC group): To disentangle the effects of congenital visual
deprivation from the effects of prevailing sensory nystagmus, which was present in all CC
participants, individuals with nystagmus due to conditions other than congenital cataracts were
tested as additional controls. Individuals in this group did not have experience a phase of severe
visual deprivation. Therefore, this group allowed us to distinguish which changes in visual
exploration behavior can be attributed to the effects of nystagmus vs congenital visual

deprivation. This group comprised of 10 participants (1 female, mean age: 15.0 years, range: 8.7 –
37.3) with Infantile Nystagmus syndrome (9 idiopathic, 1 oculocutaneous albinism), without a
history of cataracts, severe visual impairment or blindness. NC participants' visual acuity ranged
from 0.25 to 0.8 decimal units (geometrical mean: 0.45; logMar: 0.1 – 0.6, logMar mean: 0.35).

177 (4) The sighted control group (SC group) consisted of 13 individuals (3 females, mean 178 age: 23.7 years, range: 11.2 - 40.6) with normal or corrected-to-normal vision. This group was 179 partially age-matched to the CC group (no significant difference in age at testing, $t_{(21)} = -0.84$, p = 180 0.41). The SC group allowed us to establish typical eye movement parameters for healthy 181 individuals, in the current experimental setting and for the employed images.

182 All individuals were tested at the LV Prasad Eye Institute. None of the participants had any other sensory deficit or neurological disorder, diagnosed or self-reported. Expenses associated 183 184 with taking part in the study were reimbursed. Minors additionally received a small present. 185 Participants, and if applicable, their legal guardians, were informed about the study and received the instructions in one of the languages they were able to understand (in most cases Telegu, 186 187 Hindi, or English). All participants gave written informed consent before participating in the 188 study; in case of minors, legal guardians additionally provided informed consent. The study was 189 approved by the ethics board of the Faculty of Psychology and Human Movement Science of the 190 University of Hamburg (Germany) and by the ethics board of the LV Prasad Eye Institute.

191

192 Stimuli

- 193 Forty-nine images from the Natural Face and Object Stimuli image set were used in this study
- 194 (Rossion et al., 2015) (https://face-categorization-lab.webnode.com/resources/natural-face-
- 195 stimuli/). The images displayed objects representing 7 different categories: animals, chairs, fruits,
- 196 guitars, houses, plants, and telephones. Objects were located close to the center of the image.
- 197 Images were displayed in gray scale at an 800 x 800 pixel resolution, subtending 19.6 x 19.6

visual degrees. Stimuli were generated in MATLAB (The MathWorks, Natick, MA) using
Psychtoolbox 3 (Brainard, 1997; Kleiner et al., 2007) on a Windows 7 PC and presented with an
24" Eizo FG2421 LCD monitor at a resolution of 1920 x 1080 @ 120 Hz.

201Due to copyright concerns, the figures shown here use line drawings of the actual images202presented during the experiment.

203

204 Eye-tracking and calibration

205 Eye movements were recorded with a video-based binocular eye-tracking system at 500 Hz 206 (Eyelink1000 Plus, SR Research Ltd, Canada). Subjects were seated in a darkened room and 207 placed their heads on a chin rest such that their eyes were at a distance of 60 cm from the screen. 208 Due to several participants presenting nystagmus, it was not possible to use the built-in standard 209 online calibration method of the eye-tracker system. Instead, a custom-made calibration routine 210 was employed. This calibration routine used 5 screen positions as points (presented at the screen center, 15° right and left of the center and 8.5° above and below the center). Each participant was 211 212 asked to look at these 5 points. Next, the screen center position was displayed again, in order to 213 estimate calibration error. The experimenter manually controlled the calibration. During the 214 presentation of each calibration position, the experimenter decided whether an eye movement was 215 performed to the corresponding point and selected low-velocity periods of the nystagmus at each 216 calibration point. These low-velocity periods typically follow the corrective saccade of the 217 nystagmus, that is, they are aligned with the target position. The online calibration was performed to visually confirm that calibration points aligned with the 5 position patterns. This confirmation 218 219 was necessary to decide whether the procedure had to be repeated, or if the calibration was 220 sufficiently precise to continue. During offline calibration, low velocity periods of nystagmus 221 were selected as described for online calibration.

The median positions of the selected gaze samples were fitted with a polynomial function (Stampe, 1993) to the corresponding screen positions. This is the same algorithm as the one implemented in the Eyelink eye-tracker software. The same calibration procedure was applied to all participants irrespective of whether they suffered from nystagmus or not. Calibration error was calculated only for the central position of the screen, and did not differ between groups (robust linear model contrasts, all contrasts p > 0.05; mean CC group: 0.83°, SD: 0.95; mean SC group: 0.31°, SD: 0.12; mean DC group: 0.59°, SD: 0.37; mean NC group: 0.78°, SD: 0.83).

A certain proportion of gaze data was missing when the gaze fell outside of the image, or during periods when the eye tracker lost the pupil. On an average, 9.9% of CC participants' gaze data were missing, compared to 3.69% for SC, 4.27% for DC, and 9.93% for NC participants.

To guarantee a sufficiently reliable estimate, only the visual exploration data from images with at least 50% valid recordings (i.e., gaze location values within the image) were included for analyses. Under this criterion, 7, 1, 1, and 6 image explorations had to be disregarded for the CC, SC, DC and NC group, respectively. In total, we discarded less than 0.6% of the data.

236 **Procedure**

237 After the calibration was completed, the experiment was carried out in 2 blocks of 14 trials each. 238 A trial consisted of 2 images presented sequentially. Each trial started with a white fixation dot 239 (diameter $\sim 1.8^{\circ}$) presented in the center of the screen for 1 s, followed by the presentation of the 240 first image for 4 s. Next, a central white fixation dot was shown a second time for 1 s which was 241 followed by the presentation of the second image for 4 s. Participants were instructed to visually explore the images, and report the names of the objects they had encountered in the two images at 242 243 the end of the trial. After participants provided the names of the two images, the experimenter 244 decided whether each image was correctly named. The experimenters knew about the possible 245 categories and were instructed to accept responses at the exemplar level (e.g. banana) and 246 categorical level (e.g. fruit).

In 7 of the 28 trial image pairs, the same image was presented as the first and second image. In another 7 trial pairs, the two images were different, but from the same object category. In the remaining 14 trial pairs, the images were from different categories. Image presentation order was randomized across subjects with respect to pair type (repeated image, repeated category, different category). Order of presentation within a pair in the repeated- and different category pairs was randomized across subjects. The experiment took around 15-20 min, depending on the duration of the eye-tracker calibration procedure.

254

255 Data analysis and statistics

256 The common procedure in eye-tracking research is to use fixation positions as the unit of analysis. However, the nystagmus of the CC and NC individuals made it impossible to define fixations by 257 258 employing typical velocity and acceleration thresholds. Hence, the dependent variables for all 259 participants were calculated with respect to the position of all eye-tracking data samples 260 (subsequently referred to as "gaze" data, obtained at a 500 Hz sampling rate). Several studies 261 have shown that individuals with nystagmus gather information during the complete period of the 262 nystagmus, and not only during the low-velocity phase (Jin et al., 1989; Goldstein et al., 1992; 263 Waugh and Bedell, 1992; Dunn et al., 2014). Therefore, for uniformity of the analysis across 264 groups, all gaze data were used, including high-velocity samples which would normally be considered saccades. 265

266

267 Instantaneous Gaze Velocity

The extent of gaze instability in all participants was estimated by deriving "instantaneous gaze velocity". Usually, gaze velocity is calculated from multiple samples to remove high frequency noise inherent to oculomotor recordings (Stampe, 1993; Holmqvist et al., 2011). In the present study, we employed a modified version of the 2-point central difference algorithm (Bahill et al., 272 1982) that is standard in the literature (e.g., Engbert, 2003; Dimigen et al., 2009; Otero-Millan et 273 al., 2014), and used as the default by the EyeLink eye-tracker (SR Research, 2019). For a sample 274 point *n*, the corresponding instantaneous gaze velocity (visual degrees per second, $^{\circ}$ /s), is defined 275 as the sum of 6 non-consecutive eye-tracking gaze samples (position in screen pixels):

$$Velocity_{(n)} = \frac{SR \times (gaze_{(n+4)} + gaze_{(n+3)} + gaze_{(n+2)} - gaze_{(n-2)} - gaze_{(n-3)} - gaze_{(n-4)})}{18 \times PPD}$$

SR is the eye-tracker sampling rate (500 Hz), PPD the pixels-per-degree resolution (~ 40.6), and 18 corresponds to the sum of the number of samples in the intervals used in the calculation ((4--4) + (3--3) + (2--2)). This calculation was done separately for the horizontal and vertical eye movement components.

280

281 Entropy

To assess the spread or dispersion of visual exploration, the informational entropy of the spatial 282 283 distribution of gazed locations was calculated for each image and participant (Açık et al., 2010; 284 Wilming et al., 2011; Shiferaw et al., 2019). Informational entropy is defined as the average 285 amount of information of a random variable. Entropy is higher when uncertainty of an outcome is high and thus when events carry relatively more information. Entropy is maximal for variables 286 287 with a uniform distribution. In terms of visual exploration patterns, a higher spread or a broader 288 spatial distribution of gazed locations results in higher entropy. Conversely, a narrow spatial 289 distribution results in lower entropy values.

To calculate entropy values for each subject and image, first, a discrete spatial distribution of gazed locations was constructed by dividing each image into a 20 x 20 matrix of 2° x 2° cells. Next, we counted how many times each cell was gazed at by a given participant. Finally, the

293 entropy value of each spatial distribution was calculated by: $H(P) = -\sum_{i=1}^{n} \frac{p_i^{cs} * \log_2(p_i^{cs})}{Coverage(p_i^{cs})}$

where p_i^{cs} is the probability of gazing at a given cell. Coverage is a correction term suggested by Chao and Shen (2003) as a modification of the original entropy formula of Shannon in order to avoid biases due to limited sampling (Wilming et al., 2011).

In order to confirm the robustness of the results, entropy values were additionally
calculated based on gaze distributions for a smaller (1° x 1°) and larger (4° x 4°) cell size. Results
did not differ, and thus we report the results based on a cell size of 2° x 2°.

300

301 Predictor maps for visual exploration patterns

We evaluated how well each participant's exploration patterns were explained by (1) the exploration pattern of other participants; (2) by the low-level features; and (3) by the high-level visual features of the presented images. Three different predictor maps were correspondingly generated: (1) the visual exploration pattern for each image as assessed in the SC control group; (2) images' low-level Intensity Contrast Feature (ICF) model (Kümmerer et al., 2017); and (3) images' high-level feature map as defined by the DeepGaze II (DG-II) model (Kümmerer et al., 2016).

The first predictor was derived from the empirical distribution of gaze locations across all participants of the SC group. A two-dimensional spatial probability distribution was constructed for each image by pooling all the gaze eye-tracking samples of SC individuals for each image. For predictions within the SC group, the SC predictor map was constructed in a leave-one-out crossvalidation procedure. Pixel-level gaze counts were spatially smoothed with a two-dimensional Gaussian unit kernel (full width at half maximum = 2 degrees) and normalized by dividing by the total count of gaze samples.

The second predictor map, ICF, consisted of a two-dimensional spatial distribution
constructed based on the images' low-level features (luminance contrast). Different low-level

Active vision despite congenital blindness

features are known to be highly correlated (Onat et al., 2014), and simple models based on contrast features seem to perform as well as more complex models that include multiple low-level

visual features (Kienzle et al., 2009). Thus, we used a low-level model based solely on luminancecontrast.

322 The third predictor map, DG-II, consisted of a two-dimensional spatial distribution 323 constructed based on features derived by a deep neural network optimized for object recognition 324 (Simonyan and Zisserman, 2014). The DeepGaze II model is currently considered the best performing model for free viewing according to the MIT Saliency Benchmark 2019 325 326 (http://saliency.mit.edu/). The DG-II model selects local features that serve as a basis for object 327 classification, but it does not segment or tag objects. Note that the DG-II model typically 328 performs the best at predicting eye-movement behavior for images depicting text or faces, which 329 our stimuli dataset did not include. Nevertheless, the DG-II model has been shown to outperform 330 the ICF model even in the absence of such features (Kümmerer et al., 2017).

ICF and DG maps were computed for each image using the python code made available by Matthias Kümmerer and the Bethge Lab (<u>https://deepgaze.bethgelab.org</u>). ICF and DG maps were generated for each original image, as well as for three low-pass filtered image versions. The latter were obtained by filtering the images using a 2D Gaussian kernel with frequency cutoffs (0.67 reduction) at 0.5, 1, and 2 visual degrees, respectively.

336

337 Area under the curve (AUC)

To determine how well a given predictor map explained participants' visual exploration patterns, we tested whether the values of the predictor map allowed a classification of image locations as gazed versus non-gazed. For non-gazed locations, values were taken from gazed locations in other images by the same participant. This procedure to define non-gazed locations was introduced to avoid an inflated classification success due to possible spatial biases (Tatler et al., 2005; Wilming et al., 2011; Bylinskii et al., 2016), in both humans visual exploration patterns and photographic
image features (Tatler et al., 2005; Tatler, 2007; Einhäuser et al., 2008b). For each participant,
gazed and non-gazed values were pooled across images. These values were used to estimate the
classification success of a predictor map by calculating the Area Under the Curve (AUC) of the
receiver operator characteristic curve (Green and Swets, 1988; Fawcett, 2006). AUC values can
be calculated by first taking the Mann-Whitney *U* statistic (also called Wilcoxon rank-sum test)
between gazed and non-gazed values of the predictor map:

 $U = R_{gazed} - n_{gazed}(n_{gazed} + 1)/2$, where n_{gazed} is the sample size of gazed locations and R_{gazed} is the sum of ranks in the sample of gazed location, obtained by assigning a numeric rank to every gazed and non-gazed values, beginning with 1 for the smallest value. AUC values are directly derived from U by normalizing with the product of the number of gazed and non-gazed locations (Bamber, 1975):

AUC = $U/(n_{gazed} * n_{non_gazed})$. AUC values range between 0 and 1, with 0.5 corresponding to chance discrimination and 1 indicating perfect classification. In some analyses, AUC values were obtained per image rather than per subject: gazed and non-gazed values were pooled across participants for each image instead across images for each participant.

To further control for any additional potential analyzing bias, control AUC values were calculated as follows: instead of using the predictor map for a given image, images were shuffled, that is, the predictor map of another randomly selected image was used to predict visual exploration of a given image.

363

364 Statistical tests

Group differences in instantaneous gaze velocity, entropy and AUC values were evaluated withrobust linear regression models using a categorical group factor. The models employed an

Active vision despite congenital blindness

iteratively reweighted least square method using a bi-square weight function as implemented in
the MATLAB R2019b function *fitlm* (Holland and Welsch, 1977). As there were 6 possible
between-group comparisons, group contrasts were tested at a Bonferroni-corrected significance
level of 0.05/6.

Moreover, AUC values for the SC, ICF and DG-II predictor maps were evaluated for different time periods after image presentation. This analysis tested whether classification success depended on the phase of visual exploration. AUC values were computed from data partitions obtained by dividing each participant's gaze data into 8 non-overlapping 500 ms intervals, from the beginning to the end of the trial. These sets of AUC values, excluding the first interval, were entered in a linear mixed-effects model with group as a categorical factor, a time-interval covariate as a fixed effect (7 levels), and participant identity as a random effect.

In the CC and NC groups, we additionally evaluated differences in AUC values generated from gaze locations, obtained by dividing each participant's gaze data into ten bins according to the magnitude of instantaneous gaze velocity. This analysis tested whether classification success of the SC predictor map depended on gaze stability in the CC and NC group. The new set of AUC values were entered in a linear mixed-effects model with group as a categorical factor, a velocity quantile covariate as a fixed effect, and participant identity as a random effect.

To assess the effects of short-term memory on visual exploration patterns, the repetition effect was evaluated by comparing the entropy values between the first and the second image of trial pairs. Entropy values for each image were entered in a linear mixed-effects model, with participant group (4 levels: CC, SC, DC, NC) and image order within a pair (2 levels: 1st or 2nd) as fixed effect predictors, and participant identity as a random effect. This analysis was done separately for each type of trial pair (repeated identity, repeated category, unrelated new image). Linear mixed-effect models were calculated in R (version 3.6.3), using restricted

391 maximum likelihood estimation as implemented in the *lme4* package (Bates et al., 2015). The

392 reported p-values were based on the t-distribution using degrees of freedom calculated with the

393 Satterthwaites method, as implemented by the *lmerTest* package (Kuznetsova et al., 2017).

394 Differences between groups in object recognition performance were evaluated with a

395 generalized linear model using a binomial distribution and a logit link function, as implemented in

396 the R stats package. The same procedure was employed to evaluate the association between visual

397 acuity and the AUC values in CC participants. All models' detailed specifications and output

398 summaries are described in the corresponding figures' Extended data.

399

400 Open data and code accessibility

401 The code for the statistical analyses, figures, and the anonymized, pre-processed data are
402 available at the Research Data Repository of the University of Hamburg
403 (DOI:10.25592/uhhfdm.1520). Original eye-tracking datasets are available upon request from the

404 corresponding author.

405

406 **RESULTS**

407 Gaze stability is severely affected in CC participants

408 As expected from the prevailing sensory nystagmus, eye movement trajectories were considerably 409 altered in the CC group. Fig. 1a displays examples of a single trial eye-tracking recording from 410 one participant of each group (see Video 1 and Video 2 and Extended data Fig. 1-1,1-2). SC and 411 DC participants showed the prototypical gaze kinematics of visual exploration of static images: their gaze movements were characterized by periods of high stability (i.e. fixations) interrupted by 412 413 short periods of displacement at a high velocity (i.e. saccades). By contrast, CC and NC 414 participants' gaze movements were in a continuous, periodic displacement, as is typical of nystagmus. Participants' gaze stability was quantified in terms of instantaneous gaze velocity, that 415 is, how fast and in which direction the eyes moved from one moment to another (see Data 416 417 analysis and statistics – Instantaneous gaze velocity). The magnitude of instantaneous gaze 418 velocity was significantly higher in CC as compared to SC individuals (robust linear model contrast, p < 0.001, see Fig. 1b and Extended data Fig. 1-3 for the full statistic results) and DC 419 420 individuals (p < 0.001), but lower than in NC individuals (p = 0.004). Gaze velocities showed no clear direction in CC individuals, whereas for NC individuals, gaze velocities were mostly along 421 422 the horizontal direction (see Fig. 1c). Such a pattern in NC individuals is typical of horizontal jerk 423 nystagmus (Abadi and Bjerre, 2002).

In sum, these results confirm that in contrast to SC and DC participants, the gazes of CC and NC participants were in a state of continuous motion, that is, gaze stability was reduced in these two groups.

427

- 428
- 429

430 Visual exploration patterns of CC participants are stimulus-driven and similar to those of431 controls

Four examples of group-pooled exploration patterns overlaid over line drawings of the original 432 grayscale images are depicted in Fig. 2. These images illustrate the resemblance of visual 433 434 exploration patterns across groups. To quantitatively evaluate whether visual exploration patterns 435 for natural scenes were stimulus-driven in CC participants and to what degree they followed the 436 same principles as in normally sighted controls, informational entropy was derived to parametrize 437 the width of the spatial distribution of gazed locations (Shiferaw et al., 2019). Low entropy scores 438 indicate a low degree of randomness of visual exploration patterns (see Data analysis and 439 statistics – Entropy).

As expected from the nystagmus-related gaze instability, visual exploration by CC individuals covered a wider area of the images than visual exploration by SC individuals. CC participants' entropy values were higher than for SC and DC participants (robust linear model contrasts, both p < 0.001, see **Fig. 3a** and Extended data Fig. 3-1 for statistics), but not different from those of the NC participants (p = 0.27). Thus, higher entropy values in the CC group were a consequence of nystagmus, rather than of congenital visual deprivation.

Importantly, the CC group's entropy values for individual images were significantly correlated with entropy values of the same images for the three control groups (Pearson's r, all > 0.5 with p < 0.003, see **Fig. 3b**). Thus, the *relative* extent of visual exploration of images was correlated across groups. This correlation suggests that visual exploration by CC individuals was strongly dependent on the characteristics of the images, and that this dependency was qualitatively similar to the dependency on image characteristics which guided visual exploration in control individuals.

453 Since stimulus entropy assesses the extent of visual exploration, but not the precise
454 locations of gaze shifts, similar entropy values across groups do not unambiguously indicate the

455 same visual exploration patterns. Therefore, we additionally evaluated whether the exploration 456 patterns of the CC group were predicted by the corresponding visual exploration patterns of the SC group. For each image and participant, we used the pooled spatial distribution of gaze 457 locations from the SC group to create an SC predictor map. We then used the latter to predict 458 459 whether or not an image location was visually explored by CC individuals. Classification success 460 was quantified by the area under the receiver operator characteristic curve (AUC; values larger 461 than 0.5 indicate correct prediction, see *Data analysis and statistics – AUC*) (Swets, 1988; Fawcett, 2006). 462

463 SC predictor maps discriminated the CC group's gazed vs not-gazed locations above chance (all groups AUC values > 0.5, one-sample *t*-tests, p < 0.001, see Fig. 3c). In order to 464 exclude the possibility that common image characteristics or spatial biases artificially enhanced 465 466 prediction success, we ran a control analysis in which images were shuffled and AUC values from arbitrarily assigned images were derived. No successful prediction was achieved with these values 467 (none of the AUC values in either group differed from 0.5, p > 0.05). Although CC participants' 468 469 AUC values were overall lower than those for SC and DC participants (robust linear model 470 contrasts, both contrasts p < 0.001, see Extended data Fig. 3-2 for statistics), they did not differ 471 from those of the NC participants (p = 0.93).

472 In the CC group, AUC values were not correlated with visual acuity (Pearson's $r_{(8)} = -$ 473 0.19, p = 0.59, see Extended data Figure 3-3), age at testing ($r_{(8)} = -0.05$, p = 0.87), age at cataract 474 surgery ($r_{(8)} = -0.28$, p = 0.42) or time since sight restoration ($r_{(8)} = 0.2$, p = 0.56).

The previous analyses were based on the complete duration of a trial (4 s). To evaluate possible group differences in the temporal dynamics of visual exploration, we additionally ran the same analyses for the SC predictor maps separately for consecutive, non-overlapping 500 ms time intervals. For the first interval (0 to 500 ms after image presentation), all groups had low AUC values (AUC values around 0.5, see **Fig. 3d**). This result is consistent with previous findings and 480 is most likely due to the starting position being forced to be at the center of the image and thus independent of image content (Schütt et al., 2019). After the first interval, CC participants' AUC 481 482 values increased, and remained at the same level throughout image presentation. By contrast, SC, DC and NC participants reached their highest AUC values in the second interval (500 to 1000 483 484 ms), following which AUC values that progressively decreased until the end of image 485 presentation. This group difference in the dynamics of visual exploration was confirmed by a 486 mixed-effects model with a categorical predictor participant group, a time interval covariate 487 (excluding the first interval), and participant identity as random effect: CC participants' estimate of a time interval covariate was not different from 0 (p = 0.9, see Extended data Fig. 3-4 for 488 489 statistics). In other words, there was no relationship between time interval and AUC values in the 490 CC group. By contrast, all the other groups showed a significantly more negative estimate of the 491 time interval covariate than CC participants (all contrasts p < 0.006), indicating a decrease of 492 AUC values as exploration progressed in the control groups.

493 Previous research suggested that visual acuity depends on the extent of the stable, 494 "foveation", period of the nystagmus (Dell'Osso and Daroff, 1975; Dell'Osso and Jacobs, 2002; Felius et al., 2011). Therefore, it is possible that CC and NC participants mainly explore the 495 image during low-velocity periods of their nystagmus. To test this hypothesis in CC and NC 496 497 participants, AUC values were separately calculated for ten data partitions according to the 498 magnitude of the gaze instantaneous velocity (see Fig. 3e). AUC values were above chance for 499 each velocity bin. A mixed-effects model with the categorical predictor group (run only with CC 500 and NC groups), a velocity quantile covariate, and participant identity as random effect, revealed a significant effect of speed quantile (p = 0.002, see Extended data Fig. 3-5 for statistics), without 501 502 a significant main effect of group (p = 0.6) and without a significant interaction of group and the velocity quantile covariate (p = 0.83). Therefore, across both groups, slower gaze velocities 503 504 resulted in higher AUC values. The first two gaze velocity quantiles of CC and NC individuals

were roughly comparable to SC and DC individuals' instantaneous gaze velocity during fixations (see Extended data Fig. 3-6). This result suggests that CC and NC individuals were able to systematically adjust visual exploration in order to gaze at the most relevant parts of an image during the low-speed phase of the nystagmus, when visual discrimination seemed to be best in individuals with nystagmus.

Entropy and AUC values were correlated in all groups, demonstrating that the lower the spread of visual exploration, the higher the agreement of visual exploration patterns across participants (see **Fig. 3f** for the results of the CC group and Extended data Figure 3-7 for the corresponding results of the other groups). This correlation did not differ between any of the four groups (comparison of Fischer's Z-transformed *r* values, all p > 0.05).

515 In summary, CC individuals gazed at similar locations of the image as normally sighted 516 controls. These results support the hypothesis that the CC individuals' visual exploration was 517 based on the same underlying mechanisms. Thus, neither the acquisition of these representations, 518 nor their use for visual exploration via eye movements, seem to require patterned vision at birth.

519

520 Exploration patterns of CC participants are guided by both low-level and high-level visual 521 features

Next, we evaluated to what degree visual exploration patterns were guided by low-level versus high-level visual information. For this purpose, predictor maps from two different saliency models were computed for each image: A first, low-level predictor map was constructed from local contrast as defined by the Intensity Contrast Feature model (ICF) (Kümmerer et al., 2017). The second, high-level predictor map was constructed from features resulting from a deep neural network trained for object recognition, as defined by the DeepGaze II model (DG-II) (Kümmerer et al., 2016, 2017; Schütt et al., 2019).

529 In all groups, visual exploration patterns were classified above chance by both the lowlevel ICF and high-level DG-II predictor maps (see Fig. 4 a,b, all AUC > 0.5, p < 0.001). The 530 531 high-level DG-II model predicted the visual exploration patterns better (i.e., resulted in higher AUC values) than the low-level ICF model for all groups (paired t-test: CC group : p = 0.01; SC 532 group: p < 0.001; DC group: p < 0.001) except for the NC group (p = 0.13). We confirmed that 533 534 this classification accuracy was not an artifact of general image characteristics or spatial biases: 535 neither of the two models significantly predicted gaze patterns in either group after images were shuffled. These results suggest that CC individuals were able to make use of both low-level and 536 537 high-level visual information for guiding visual exploration, similar to SC individuals.

538 AUC values were overall lower in the CC group compared to the SC and DC group for 539 both low- and high-level predictor maps (robust linear model contrasts, all p < 0.004, see Fig. 4 540 **a,b** and Extended data Fig. 4-1 and 4-2 for statistics), while they did not significantly differ from 541 the corresponding AUC values of the NC group (both p > 0.05). Importantly, the relative 542 predictive power of the two models (ratio of the ICF and DG-II AUC values) was 543 indistinguishable between the CC group and the three control groups (all p > 0.05, see Fig. 4c and Extended data Fig. 4-3 for statistics). This confirmed that CC individuals weighted low- and high-544 level visual information for guiding visual exploration similar to the SC, NC and DC groups. 545

546 As in the analysis for the SC predictor map, we ran the analyses for the ICF and DG-II predictor maps separately for consecutive time intervals (see Extended data Fig. 4-4). For the 547 548 low-level ICF predictor, the time interval covariate was not significant in any group (estimate not 549 different from 0, all p > 0.1, see Extended data Fig. 4-5 for statistics). For the high-level DG-II 550 predictor, the SC group showed an effect of interval (p < 0.001). By contrast, this effect was non-551 significant in the CC (p = 0.29), DC (p = 0.06) or NC (p = 0.12) groups. Nevertheless, the 552 estimate of the time interval covariate was more negative in the SC and DG group than in the CC 553 group (p < 0.0002 and p < 0.04 respectively, see Extended data Fig. 4-6 for statistics).

554 Additionally, AUC values obtained from saliency predictor maps computed from low-pass filtered images explained visual exploration in the CC and NC groups better than in the SC and 555 DC groups (see Extended data Figure 4-7, and 4-8 and 4-9 for statistics). This is consistent with 556 CC and NC individuals' reduced visual acuity and reduced sensitivity to higher spatial 557 frequencies (Ellemberg et al., 1999; Bedell, 2006; Hertle and Reese, 2007). Thus, it is justified to 558 559 conclude that CC and NC individuals' visual exploration predominantly made use of the low 560 rather than high spatial frequency components of visual stimulus features. 561 In sum, these results demonstrate a highly preserved ability of CC individuals to use both 562 low-and high-level visual information to guide visual exploration.

563

564 Changes in visual exploration patterns for repeated images indicate visual short-term 565 memory effects in CC individuals

Visual exploration patterns narrow down after an image has been repeatedly encountered (Noton and Stark, 1971; Ryan et al., 2000; Smith et al., 2006; Kaspar and König, 2011). This result has been taken as evidence for visual exploration being guided not only by stimulus-driven but additionally by top-down factors. In order to assess such short-term memory effects, we analyzed differences in gaze entropy for two consecutive images, for which the second image was either (1) identical to the first image, (2) a different image but displaying an item of the same category as the first image or (3) a different, unrelated image.

Entropy values decreased between the first and second presentation of the same image in all groups, including the CC group (see **Fig. 5a**). Furthermore, this reduction in the spread of visual exploration between repeated images did not differ between groups (no significant interaction between image repetition and group, p > 0.05, see Extended data Fig. 5-1 for statistics). Importantly, in all groups, the reduction in entropy for consecutive images was specific for repeated images and did not generalize to category repetitions or different images (see Fig. 5a
and Extended data Figure 5-2,3 for statistics).

In summary, CC individuals' visual exploration patterns showed the same short-term memory related reduction in spread as found in the control groups and demonstrated in previous research (Noton and Stark, 1971; Ryan et al., 2000; Smith et al., 2006; Kaspar and König, 2011). This result suggests that CC individuals are able to integrate both stimulus-driven and top-down information from short-term memory, in order to guide visual exploration.

585

587

586 Object recognition performance is linked to systematic visual exploration in CC individuals

Object recognition performance was high in all groups (see Fig. 5b). All SC participants,

588 independent of their chronological age at testing, performed at 100%. Overall, the performance of 589 the CC group (mean: 84,2% correct, range 30.3-100%) was lower than in the three other groups 590 (p < 0.001; see Extended data Fig. 5-4 for statistics). For CC participants, a logistic regression 591 model analysis revealed that object recognition performance was associated with better visual acuity (visual acuity predictor, p < 0.001, see Fig 5c and Extended data Fig. 5-5 for statistics) but 592 593 not with age at testing (see Extended data Figure 5-6,7). Crucially, object recognition was 594 additionally related to how well the CC individuals' exploration patterns were predicted by the 595 exploration patterns of SC participants (AUC predictor, p < 0.001). According to AIC and Tjur R² 596 model-fit metrics (see Extended data Fig. 5-5), a model with both the visual acuity and AUC 597 predictors performed better at explaining the object recognition scores of CC individuals than a 598 model with either predictor in isolation. While high overall object recognition performance in CC 599 individuals is in accordance with previous findings (Ostrovsky et al., 2009; Röder et al., 2013), 600 this result further suggests that object recognition performance in CC individuals might benefit 601 from systematic visual exploration.

602

603 **DISCUSSION**

Visual exploration of natural scenes by means of eye movements is guided by stimulus-driven 604 605 mechanisms that make use of low- and high-level visual features as well as by top-down mechanisms such as explicit goals and memory representations. The present study investigated 606 607 the degree to which the development of the bottom-up and top-down mechanisms guiding 608 systematic visual exploration of natural stimuli relies on early visual experience. Here, we tested 609 visual exploration patterns in 10 individuals who had received delayed treatment for total dense bilateral congenital cataracts (CC group), some of whom only in late childhood or adulthood. 610 Participants watched close-up photographic images of different objects, plants, animals and 611 buildings. The visual exploration patterns of CC individuals were compared to those of a group of 612 613 normally sighted controls (SC group), individuals treated for late-onset cataracts (DC group), and 614 a group of individuals with pathological nystagmus, but without a history of congenital cataracts 615 or visual deprivation (NC group). We found remarkably preserved visual exploration behavior in 616 the CC group, despite an absence of visual experience early in life. Indeed, CC individuals' visual 617 exploration patterns were successfully predicted by those of the SC group. The application of 618 modelling approaches to identify the visual features guiding visual exploration revealed that CC 619 individuals employed both low-level and high-level visual information, and did so with a similar 620 relative weighting as observed in the control groups. Furthermore, by analyzing the effects of 621 short-term memory on visual exploration patterns, we demonstrated that CC individuals were able 622 to integrate recently acquired memory representations with stimulus-driven visual information. 623 Finally, despite the high object recognition scores of CC individuals, residual deficits were associated not only with their persistent lower visual acuity, but additionally were associated with 624 625 the degree to which their visual exploration patterns resembled those of typically sighted 626 individuals.

627 While most studies in sight-recovery individuals have focused on visual perceptual 628 functions, the interaction of the visual and oculomotor system has hardly ever been investigated in 629 this population. On one hand, this is surprising, given that visual perception crucially depends on overt exploration to align the gaze with the most relevant regions of the visual world. On the other 630 hand, eye movements of sight-recovery individuals born with severe visual impairment or 631 632 blindness are highly distorted due to a superimposing involuntary nystagmus, making them harder 633 to assess (Abadi et al., 2006). The emergence of nystagmus in CC individuals is a direct consequence of visual deprivation within the first 8-12 weeks of life; the first 12 weeks of life are 634 635 considered a sensitive period for the development of gaze stability control (Rogers et al., 1981; 636 Gelbart et al., 1982; Lambert et al., 2006; Birch et al., 2009). We observed more irregular 637 nystagmus in CC individuals than in NC individuals, whose nystagmus patterns of horizontal jerk 638 movements with accelerating slow phases were characteristic of Infantile Nystagmus syndrome. 639 While Abadi et al. (2006) did not directly demonstrate such irregularities in the nystagmus pattern 640 of CC individuals, their study reported that, in accordance with our observations, more irregular 641 nystagmus, that is, with multiplanar rather than uniplanar patterns, seems to emerge in severe 642 cases of congenital cataracts.

643 To the best of our knowledge, the present study is the first demonstration that individuals 644 with nystagmus, regardless of etiology, are able to systematically explore natural images despite 645 nystagmus related distortions. Previous research suggested that visual acuity in individuals with nystagmus depends on the duration of the "foveation" periods within their nystagmus (Dell'Osso 646 647 and Daroff, 1975; Dell'Osso and Jacobs, 2002; Felius et al., 2011). In both the CC and NC groups, we observed that exploration was more predictable during low-velocity periods, that is 648 649 during periods which by and large resemble foveation periods. Thus, individuals with nystagmus 650 are capable of taking into account their idiosyncratic nystagmus pattern while exploring an image. 651 However, it needs to be stressed that visual exploration was predictable in both the CC and the

NC groups for the complete range of gaze velocities. This result is in agreement with more recent
research on visual acuity during nystagmus, which indicated that visual perception is possible
throughout the nystagmus cycle (Dunn et al., 2014).

655 While a qualitative assessment of simple ocular orienting to light is routinely performed in CC individuals during clinical examination, the presence of nystagmus has made it difficult to 656 657 quantitatively study systematic eye movement behavior in this group. It was only recently that 658 visually guided behavior was successfully assessed with eye tracking in CC individuals (Zerr et 659 al., 2020). In this study, participants followed a salient, single, visual target which abruptly but 660 regularly changed location. CC individuals showed intact visually guided eye movements, which were as precise and as fast as can be expected after taking their nystagmus into account. While 661 such visually guided eye movements are likely a prerequisite for the exploration of natural scenes, 662 663 they might be accounted for, to a large degree, by a simple reflexive mechanism based on luminance contrast. By contrast, real-world visual exploration is not just driven by low-level 664 665 information such as luminance contrast, but additionally uses high-level features, and integrates top-down influences such as goals and prior knowledge retrieved from memory (Tatler et al., 666 667 2011; König et al., 2016; Veale et al., 2017). Since previous research has documented better recovery of low-level than high-level visual processing in CC individuals (McKyton et al., 2015; 668 669 Sourav et al., 2020; Pitchaimuthu et al., 2021), we expected that visual exploration of natural 670 images would be mostly guided by low-level visual features. Contrary to this hypothesis, CC 671 individuals relied on high-level information, and used both low- and high-level information in a 672 similar manner to SC and DC control groups.

For all three predictor maps (SC group predictor maps, ICF and DG-II predictors), the AUC values were significantly higher than chance in predicting the gaze patterns of CC individuals. However, they were overall lower than what has often been reported in similar studies (Wilming et al., 2011; Bylinskii et al., 2016; Kümmerer et al., 2017). This might be due to

the characteristics of the images and constraints of the present study. First, all images featured a 677 678 single central object, which might have reinforced a visual exploration bias towards the center. 679 Since our analysis procedure controlled for this potential central bias, it might have lowered AUC values in the present study. Second, grayscale images were presented, which attenuated features 680 681 that strongly guide typical visual exploration (Onat et al., 2014). Third, our analysis was not based 682 only on fixations, but rather considered all eye-tracking gaze samples of the complete trial, 683 including saccades. This was necessary due to the prevailing nystagmus in the CC and NC groups, and for a uniformity of the analysis across groups. By contrast, almost all previous studies 684 685 that evaluate free-viewing behavior are based on fixations excluding saccades, and often 686 excluding the first fixation following image presentation.

687 Although we found overall broader and less well-predicted visual exploration patterns in 688 the CC group than in the SC and DC group, CC participants' visual exploration was overall 689 comparable to visual exploration in the NC group. A difference between the CC and NC groups 690 was however detected in a time interval resolved analysis: Whereas in SC, DC, and NC 691 participants exploration was more predictable at the beginning of visual exploration (500 to 1000 692 ms interval) than during later phases, CC participants showed consistent AUC values throughout 693 the exploration period. Decreasing predictability of visual exploration has been observed in 694 previous research (Onat et al., 2014; Schütt et al., 2019). This has been interpreted as an initial 695 bottom-up orienting response, followed by a gradual broadening of visual exploration (Schütt et 696 al., 2019). The initial strong bottom-up response has been shown to be a consequence of the use 697 of high-level, rather than primary low-level features (Onat et al., 2014; Schütt et al., 2019). Indeed, this is the pattern of visual exploration that was observed in the SC group. In contrast to 698 699 the SC group, prediction accuracy driven by high-level features did not vary with time in the CC 700 individual. Thus, we speculate that despite using high level features for visual guidance, high-701 level information did not interact with the initial phase of bottom-up exploration in the CC group. Future research might confirm this observation, since the dynamic change of predictability of thehigh-level model was not significant in the DC and NC groups.

It is unclear to which degree CC individuals are capable of visually exploring more complex scenes, e.g. images with multiple items, or images which are generally harder to perceive for them. In fact, as a recent study has reported that CC individuals conduct fewer eye movements to the eyes region (Zohary et al., 2022). In the present study we also avoided high stimulus eccentricities due to well-known deficits in peripheral vision of CC individuals (Lewis and Maurer, 2005), which is likely enhanced by the effects of nystagmus (Chung and Bedell, 1995; Pascal and Abadi, 1995).

711 Stimulus-driven guidance of visual exploration is thought to emerge from topographical 712 "feature maps" representing visual features such as color, orientation, luminance, and motion (Itti 713 and Koch, 2001; Veale et al., 2017). It is assumed that these feature maps serve as a source for 714 "saliency maps." Saliency maps represent how conspicuous or "salient" different regions of the 715 visual field might be (Koch and Ullman, 1985; Itti and Koch, 2000). Our results indicated that the 716 emergence of both of these mechanisms - the extraction of visual feature maps as well as the 717 computation of saliency maps - do not seem to depend on early visual experience during a 718 sensitive period.

719 The computation of feature and saliency maps has been proposed to be followed by the 720 derivation of a "priority map" (Bisley and Goldberg, 2010). Priority maps are thought to combine 721 bottom-up stimulus-driven information and top-down constrains, in order to select the next gaze 722 location (Bisley and Goldberg, 2010; Veale et al., 2017). Top down influences have often been studied by manipulating task instructions. A special case of a non-reflexive, implicit top-down 723 724 influence on visual exploration is the effect of short-term memory: If an image is repeated, the 725 distribution of gazed locations narrows down (Hannula, 2010). Short-term memory effects on 726 visual exploration due to image repetition have been reported to be unrelated to changes in low127 level visual features (Kaspar and Konig, 2011), suggesting that these effects are neither due to 128 low-level adaptation, nor due to a reweighting of low- and high-level image features. Whether or 129 not the CC group would show memory-based gains on visual exploration over longer delay 130 periods, as used in previous studies (Hannula, 2010), or other task based top-down effects, might 131 be investigated in future studies.

732 CC participants were able to recognize the visual stimuli, in agreement with previous 733 reports showing that even after a long period of congenital blindness, sight-recovery individuals 734 were able to correctly name everyday objects (Maurer et al., 2005; Ostrovsky et al., 2009; Röder 735 et al., 2013) and to recognize artificial objects through temporal integration (Orlov et al., 2021). 736 In contrast to normally sighted participants who performed at ceiling, the CC group's 737 performance on object recognition was not perfect in the present study. Crucially, better image 738 recognition in CC individuals was associated not only with better visual acuity, but additionally 739 with how much CC participants' gaze patterns resembled those of normally sighted controls. 740 Although this association must be considered preliminary due to the limited sample size in the 741 present study, this finding is compatible with previous research. For ambiguous or noisy stimuli, 742 visual exploration of diagnostic features precedes explicit recognition, rather than object 743 recognition guiding exploration (Holm et al., 2008; Kietzmann et al., 2011). The currently 744 available data do not allow us to draw conclusions about whether object recognition is as fast in 745 CC individuals as in controls. However, similar latencies of the N170 wave of event-related 746 potentials, an electrophysiological component which has been associated with the structural 747 encoding of objects, speaks in favor for a recovery of typical object recognition times in CC 748 individuals (Röder et al., 2013). Since the overall low visual acuity in CC individuals can be 749 considered analogous to noise, we speculate that visual exploration aided rather than interfered 750 with object recognition in CC individuals.

Active vision despite congenital blindness

751 The idea that visual exploration promotes object recognition is reminiscent of theories 752 from developmental psychology on how infants learn to recognize objects. For example, 753 information processing accounts assume that object recognition emerges in an active interaction with the visual world (Johnson and Johnson, 2000; Johnson, 2001; Johnson et al., 2008). Object 754 755 recognition advances with an improvement in active sampling, that is, in visual exploration. It has 756 been hypothesized that newborns' preference for edges and motion, as well as their ability for 757 figure-ground segregation, acts as an initial guide for where to look (Slater et al., 1990; Johnson 758 and Johnson, 2000; Johnson, 2001). Further, it was proposed that object-defining higher-level features are acquired while continuously exploring the visual world (Johnson and Johnson, 2000). 759 760 For example, the level of object knowledge in 2-3.5 month old infants (Johnson et al., 2004) and 761 the ability to process facial expressions in 6-11 month old infants (Amso et al., 2010) were found 762 to depend on visual exploration patterns. Our results are consistent with the idea of active visual 763 exploration being instrumental for the acquisition of object knowledge. We speculate that CC 764 individuals' post-surgery visual exploration might initially have made use of the same preferences 765 for edges and motion as suggested for newborns (Johnson and Johnson, 2000; Johnson, 2001). 766 This additionally requires functioning oculomotor control in CC individuals, capable of taking nystagmus related trajectories into account. As children refine visual exploration to rely more on 767 768 high-level features (Açık et al., 2010; Helo et al., 2014), we assume the same for CC individuals 769 following cataract removal surgery. Indeed, CC individuals of the present study who had acquired 770 the most typical visual exploration patterns were those who performed the best at object 771 recognition.

None of the measures tested (i.e., entropy, AUC, and performance) showed an association with age at testing or time since surgery in CC participants. At first glance, this result seems surprising given the large range of ages at testing and of time passed since surgery. However, the lack of such a significant association requires replication, since our sample size was limited by the

Active vision despite congenital blindness

776 availability of a rare population. Further, all CC participants were older than 10 years of age. 777 Previous research has reported adult like visual exploration in terms of entropy and AUC 778 measures in children older than 7 years of age (Açık et al., 2010; Helo et al., 2014). Finally, we 779 tested CC individuals at least 7 months post-surgery. Thus, the duration since surgery within 780 which visual input was available might have been sufficient to acquire visual exploration 781 strategies, and the associated object knowledge. In fact, previous research in cataract-reversal 782 individuals who underwent a long period of visual deprivation has provided evidence that 783 knowledge of object shape emerges within this time period (Wright et al., 1992; Ostrovsky et al., 2009; Held et al., 2011; Chen et al., 2016). 784

785 In conclusion, the remarkably preserved exploration patterns of sight-recovery individuals 786 with a history of a transient phase of congenital patterned visual deprivation suggests that the 787 development of visual exploration mechanisms does not depend on experience within a sensitive 788 period. In contrast to prevailing deficits in visual acuity, gaze stability, and other high-level visual 789 functions (Röder and Kekunnaya, 2021b), visual exploration mechanisms seem to emerge after 790 sight restoration. We speculate that similar to infants, the newly available, low spatial frequency 791 information might initiate recovery in individuals with reversed congenital cataract; followed by 792 refinement, as in typical ontogenetic development. Finally, it might be hypothesized that visual 793 exploration after sight restoration surgery might stimulate the acquisition of visual object 794 knowledge despite visual acuity deficits and nystagmus.

795

796 **REFERENCES**

- Abadi RV, Bjerre A (2002) Motor and sensory characteristics of infantile nystagmus. The British
 journal of ophthalmology 86:1152–1160.
- Abadi RV, Forster JE, Lloyd IC (2006) Ocular motor outcomes after bilateral and unilateral
 infantile cataracts. Vision Research 46:940–952.
- Açık A, Onat S, Schumann F, Einhäuser W, König P (2009) Effects of luminance contrast and its modifications on fixation behavior during free viewing of images from different categories. Vision research 49:1541–1553.
- Açık A, Sarwary A, Schultze-Kraft R, Onat S, König P (2010) Developmental changes in natural
 viewing behavior: Bottomup and top-down differences between children, young adults
 and older adults. Frontiers in Psychology 1:207.
- Amso D, Fitzgerald M, Davidow J, Gilhooly T, Tottenham N (2010) Visual Exploration Strategies
 and the Development of Infants' Facial Emotion Discrimination. Frontiers in Psychology
 1:180.
- 811 Bahill AT, Kallman JS, Lieberman JE (1982) Frequency limitations of the two-point central 812 difference differentiation algorithm. Biol Cybern 45:1–4.
- 813 Bamber D (1975) The area above the ordinal dominance graph and the area below the receiver 814 operating characteristic graph. Journal of Mathematical Psychology 12:387–415.
- Bates D, Mächler M, Bolker B, Walker S (2015) Fitting Linear Mixed-Effects Models Using Ime4.
 Journal of Statistical Software 67 Available at: http://www.jstatsoft.org/v67/i01/.
- Bedell HE (2006) Visual and Perceptual Consequences of Congenital Nystagmus. Seminars in
 Ophthalmology 21:91–95.
- Birch EE, Cheng C, Stager DR, Weakley DR, Stager DR (2009) The critical period for surgical
 treatment of dense congenital bilateral cataracts. Journal of American Association for
 Pediatric Ophthalmology and Strabismus 13:67–71.
- Bisley JW, Goldberg ME (2010) Attention, intention, and priority in the parietal lobe. Annual
 review of neuroscience 33:1–21.
- 824 Brainard DH (1997) The psychophysics toolbox. Spatial vision 10:433–436.
- Bylinskii Z, Judd T, Oliva A, Torralba A, Durand F (2016) What do different evaluation metrics tell
 us about saliency models? arXiv:160403605 [cs].
- Chen J, Wu E-D, Chen X, Zhu L-H, Li X, Thorn F, Ostrovsky Y, Qu J (2016) Rapid Integration of
 Tactile and Visual Information by a Newly Sighted Child. Current Biology 26:1069–1074.
- Chung STL, Bedell HE (1995) Effect of retinal image motion on visual acuity and contour
 interaction in congenital nystagmus. Vision Research 35:3071–3082.
- Bell'Osso LF, Daroff RB (1975) Congenital nystagmus waveforms and foveation strategy.
 Documenta Ophtalmologica 39:155–182.

eNeuro Accepted Manuscript 847

833

834

Intersubject Prediction of Best-Corrected Visual Acuity. Documenta Ophtalmologica 835 104:28. 836 Dimigen O, Valsecchi M, Sommer W, Kliegl R (2009) Human microsaccade-related visual brain 837 responses. The Journal of Neuroscience 29:12321-12331. 838 Dunn MJ, Margrain TH, Woodhouse JM, Ennis FA, Harris CM, Erichsen JT (2014) Grating visual 839 acuity in infantile nystagmus in the absence of image motion. Investigative 840 Ophthalmology and Visual Science 55:2682-2686. 841 Eckstein MP (2011) Visual search: A retrospective. Journal of Vision 11:14-14. 842 Einhauser W, Martin KAC, Konig P (2004) Are switches in perception of the Necker cube related 843 to eye position? European Journal of Neuroscience 20:2811-2818. 844 Einhäuser W, Rutishauser U, Koch C (2008a) Task-demands can immediately reverse the 845 effects of sensory-driven saliency in complex visual stimuli. Journal of vision 8:2.1-19. 846 Einhäuser W, Spain M, Perona P (2008b) Objects predict fixations better than early saliency.

Dell'Osso LF, Jacobs JB (2002) An Expanded Nystagmus Acuity Function: Intra- and

848 Ellemberg D, Lewis TL, Maurer D, Hong Lui C, Brent HP (1999) Spatial and temporal vision in 849 patients treated for bilateral congenital cataracts. Vision Research 39:3480-3489.

Journal of vision 8:18.1-26.

- 850 Engbert R (2003) Microsaccades uncover the orientation of covert attention. Vision Research 851 43:1035-1045.
- 852 Fawcett T (2006) An introduction to ROC analysis. Pattern Recognition Letters 27:861–874.
- 853 Felius J, Fu VLN, Birch EE, Hertle RW, Jost RM, Subramanian V (2011) Quantifying Nystagmus 854 in Infants and Young Children: Relation between Foveation and Visual Acuity Deficit. 855 Investigative Opthalmology & Visual Science 52:8724.
- 856 Ganesh S, Arora P, Sethi S, Gandhi TK, Kalia A, Chatterjee G, Sinha P (2014) Results of late 857 surgical intervention in children with early-onset bilateral cataracts. British Journal of 858 Ophthalmology 98:1424-1428.
- 859 Gelbart SS, Hoyt CS, Jastrebski G, Marg E (1982) Long-Term Visual Results in Bilateral 860 Congenital Cataracts. American Journal of Ophthalmology 93:615-621.
- 861 Goldstein HP, Gottlob I, Fendick MG (1992) Visual remapping in infantile nystagmus. Vision 862 Research 32:1115-1124.
- 863 Green DM, Swets JA (1988) Signal Detection Theory and Psychophysics. Peninsula Pub.
- 864 Hannula DE (2010) Worth a glance: using eye movements to investigate the cognitive 865 neuroscience of memory. Frontiers in Human Neuroscience 4:166.
- Held R, Ostrovsky Y, de Gelder B, Gandhi T, Ganesh S, Mathur U, Sinha P (2011) The newly 866 867 sighted fail to match seen with felt. Nat Neurosci 14:551-553.
- 868 Helo A, Pannasch S, Sirri L, Rämä P (2014) The maturation of eye movement behavior: Scene 869 viewing characteristics in children and adults. Vision Research 103:83-91.

- Hensch TK (2005) Critical period plasticity in local cortical circuits. Nature Reviews Neuroscience
 6:877–888.
- Hertle RW, Reese M (2007) Clinical contrast sensitivity testing in patients with infantile
 nystagmus syndrome compared with age-matched controls. American journal of
 ophthalmology 143:1063–1065.
- Holland PW, Welsch RE (1977) Robust regression using iteratively reweighted least-squares.
 Communications in Statistics Theory and Methods 6:813–827.
- Holm L, Eriksson J, Andersson L (2008) Looking as if you know: Systematic object inspection
 precedes object recognition. Journal of Vision 8:14.
- Holmqvist K, Nyström M, Andersson R, Dewhurst R, Jarodzka H, van de Weijer J (2011) Eye
 Tracking: A comprehensive guide to methods and measures. OUP Oxford.
- Itti L, Koch C (2000) A Saliency-Based Search Mechanism for Overt and Covert Shifts of Visual
 Attention. Vision Research 40:1489–1506.
- 883 Itti L, Koch C (2001) Computational modelling of visual attention. Nature Reviews Neuroscience
 884 2:194–203.
- Jin YH, Goldstein HP, Reinecke RD (1989) Absence of visual sampling in infantile nystagmus.
 Korean J Ophthalmol 3:28–32.
- Johnson SP (2001) Visual development in human infants: Binding features, surfaces, and
 objects. Visual Cognition 8:565–578.
- Johnson SP, Davidow J, Hall-Haro C, Frank MC (2008) Development of perceptual completion
 originates in information acquisition. Developmental Psychology 44:1214–1224.
- Johnson SP, Johnson KL (2000) Early perception-action coupling: eye movements and the
 development of object perception. Infant Behavior and Development 23:461–483.
- Johnson SP, Slemmer JA, Amso D (2004) Where Infants Look Determines How They See: Eye
 Movements and Object Perception Performance in 3-Month-Olds. Infancy 6:185–201.
- Kaspar K, König P (2011) Overt Attention and Context Factors: The Impact of Repeated
 Presentations, Image Type, and Individual Motivation. PLoS ONE 6:e21719.
- Kaspar K, Konig P (2011) Viewing behavior and the impact of low-level image properties across
 repeated presentations of complex scenes. Journal of Vision 11:26–26.
- Kienzle W, Franz MO, Schölkopf B, Wichmann F a (2009) Center-surround patterns emerge as
 optimal predictors for human saccade targets. Journal of vision 9:7.1-15.
- Kietzmann TC, Geuter S, König P (2011) Overt Visual Attention as a Causal Factor of Perceptual
 Awareness. PloS one 6:e22614.
- Kleiner M, Brainard D, Pelli D (2007) What's new in Psychtoolbox-3? Perception ECVP abstract
 36.
- Knudsen EI (2004) Sensitive Periods in the Development of the Brain and Behavior. Journal of
 Cognitive Neuroscience 16:1412–1425.

- Koch C, Ullman S (1985) Shifts in selective visual attention: towards the underlying neural
 circuitry. Human neurobiology 4:219–227.
- König P, Wilming N, Kietzmann TC, Ossandón JP, Onat S, Ehinger BV, Gameiro RR, Kaspar K
 (2016) Eye movements as a window to cognitive processes. Journal of Eye Movement
 Research 9:1–16.
- Kümmerer M, Wallis TSA, Bethge M (2016) DeepGaze II: Reading fixations from deep features
 trained on object recognition. arXiv:161001563.
- Kümmerer M, Wallis TSA, Gatys LA, Bethge M (2017) Understanding Low- and High-Level
 Contributions to Fixation Prediction. In: 2017 IEEE International Conference on Computer
 Vision (ICCV), pp 4799–4808. Venice: IEEE.
- 817 Kuznetsova A, Brockhoff PB, Christensen RHB (2017) ImerTest Package: Tests in Linear Mixed
 818 Effects Models. Journal of Statistical Software 82 Available at:
 919 http://www.jstatsoft.org/v82/i13/.
- Lambert SR, Lynn MJ, Reeves R, Plager DA, Buckley EG, Wilson ME (2006) Is There a Latent
 Period for the Surgical Treatment of Children With Dense Bilateral Congenital Cataracts?
 Journal of American Association for Pediatric Ophthalmology and Strabismus 10:30–36.
- Le Grand R, Mondloch CJ, Maurer D, Brent HP (2001) Early Visual Experience and Face
 Processing. Nature 412:26–27.
- Lewis TL, Maurer D (2005) Multiple sensitive periods in human visual development: Evidence
 from visually deprived children. Developmental Psychobiology 46:163–183.
- Maurer D, Lewis TL, Mondloch CJ (2005) Missing sights: Consequences for visual cognitive
 development. Trends in Cognitive Sciences 9:144–151.
- 929 Maurer D, Mondloch CJ, Lewis TL (2007) Sleeper effects. Developmental Science 10:40-47.
- 930McKyton A, Ben-Zion I, Doron R, Zohary E (2015) The Limits of Shape Recognition following931Late Emergence from Blindness. Current Biology 25:2373–2378.
- Noton D, Stark L (1971) Scanpaths in Eye Movements during Pattern Perception. Science
 171:308–311.
- Nuthmann A, Henderson JM (2010) Object-based attentional selection in scene viewing. Journal
 of vision 10:20.
- Onat S, Açık A, Schumann F, König P (2014) The contributions of image content and behavioral
 relevancy to overt attention. PLoS ONE 9:e93254.
- Orlov T, Raveh M, McKyton A, Ben-Zion I, Zohary E (2021) Learning to perceive shape from
 temporal integration following late emergence from blindness. Current Biology 31:3162 3167.e5.
- 941Ostrovsky Y, Meyers E, Ganesh S, Mathur U, Sinha P (2009) Visual Parsing After Recovery942From Blindness. Psychological Science 20:1484–1491.
- Otero-Millan J, Castro JLA, Macknik SL, Martinez-Conde S (2014) Unsupervised clustering
 method to detect microsaccades. Journal of Vision 14:18–18.

- Pascal E, Abadi RV (1995) Contour interaction in the presence of congenital nystagmus. Vision
 research 35:1785–1789.
- Pitchaimuthu K, Dormal G, Sourav S, Shareef I, Rajendran SS, Ossandón JP, Kekunnaya R,
 Röder B (2021) Steady state evoked potentials indicate changes in nonlinear neural
 mechanisms of vision in sight recovery individuals. Cortex 144:15–28.
- Putzar L, Hötting K, Röder B (2010) Early visual deprivation affects the development of face
 recognition and of audio-visual speech perception. Restorative Neurology and
 Neuroscience 28:251–257.
- Putzar L, Hötting K, Rösler F, Röder B (2007) The development of visual feature binding
 processes after visual deprivation in early infancy. Vision Research 47:2616–2626.
- Röder B, Kekunnaya R (2021a) Visual experience dependent plasticity in humans. Curr Opin
 Neurobiol 67:155–162.
- Röder B, Kekunnaya R (2021b) Visual experience dependent plasticity in humans. Current
 Opinion in Neurobiology 67:155–162.
- Röder B, Ley P, Shenoy BH, Kekunnaya R, Bottari D (2013) Sensitive periods for the functional
 specialization of the neural system for human face processing. Proceedings of the
 National Academy of Sciences 110:16760–16765.
- Rogers GL, Tishler CL, Tsou BH, Hertle RW, Fellows RR (1981) Visual Acuities in Infants With
 Congenital Cataracts Operated on Prior to 6 Months of Age. Archives of Ophthalmology
 99:999–1003.
- Rossion B, Torfs K, Jacques C, Liu-Shuang J (2015) Fast periodic presentation of natural
 images reveals a robust face-selective electrophysiological response in the human brain.
 Journal of Vision 15:18–18.
- Ryan JD, Althoff RR, Whitlow S, Cohen NJ (2000) Amnesia is a Deficit in Relational Memory.
 Psychological Science 11:454–461.
- Schulze-Bonsel K, Feltgen N, Burau H, Hansen L, Bach M (2006) Visual Acuities "Hand Motion"
 and "Counting Fingers" Can Be Quantified with the Freiburg Visual Acuity Test.
 Investigative Opthalmology & Visual Science 47:1236.
- Schütt HH, Rothkegel LOM, Trukenbrod HA, Engbert R, Wichmann FA (2019) Disentangling
 bottom-up versus top-down and low-level versus high-level influences on eye movements
 over time. Journal of Vision 19:1.
- 976Shiferaw B, Downey L, Crewther D (2019) A review of gaze entropy as a measure of visual977scanning efficiency. Neuroscience & Biobehavioral Reviews 96:353–366.
- Simonyan K, Zisserman A (2014) Very Deep Convolutional Networks for Large-Scale Image
 Recognition. arXiv:14091556 [cs].
- Slater A, Morison V, Somers M, Mattock A, Brown E, Taylor D (1990) Newborn and older infants'
 perception of partly occluded objects. Infant Behavior and Development 13:33–49.
- Smith CN, Hopkins RO, Squire LR (2006) Experience-Dependent Eye Movements, Awareness,
 and Hippocampus-Dependent Memory. Journal of Neuroscience 26:11304–11312.

Sourav S, Bottari D, Shareef I, Kekunnaya R, Röder B (2020) An electrophysiological biomarker
 for the classification of cataract-reversal patients: A case-control study. EClinicalMedicine
 27:100559.

- 987 SR Research (2019) Models of Velocity and Acceleration Calculations. In: Experiment Builder
 988 2.2.1 [Computer software]. Mississauga, Ontario, Canada: SR Research Ltd.
- Stampe DM (1993) Heuristic filtering and reliable calibration methods for video-based pupil tracking systems. Behavior Research Methods, Instruments, & Computers 25:137–142.
- 991 Swets JA (1988) Measuring the Accuracy of Diagnostic Systems. Science 240:1285–1293.
- Tatler BW (2007) The central fixation bias in scene viewing: Selecting an optimal viewing
 position independently of motor biases and image feature distributions. Journal of Vision
 7:1–17.
- Tatler BW, Baddeley R, Gilchrist I (2005) Visual correlates of fixation selection: effects of scale and time. Vision research 45:643–659.
- Tatler BW, Hayhoe M, Land M, Ballard D (2011) Eye guidance in natural vision: Reinterpreting salience. Journal of vision 11:1–23.
- Veale R, Hafed ZM, Yoshida M (2017) How is visual salience computed in the brain? Insights
 from behaviour, neurobiology and modelling. Philosophical Transactions of the Royal
 Society B: Biological Sciences 372:20160113.
- Waugh SJ, Bedell HE (1992) Sensitivity to Temporal Luminance Modulation in Congenital
 Nystagmus. Investigative Ophthalmology & Visual Science 33:9.
- Wilming N, Betz T, Kietzmann TC, König P (2011) Measures and Limits of Models of Fixation Selection. PloS one 6:e24038.
- World Health Organization (2019) Vision impairment. In: World report on vision (Gilbert C, Jackson ML, Kyari F, Naidoo K, Rao GN, Resnikoff S, West S, eds), pp 10–16. World Health Organization. Available at: https://apps.who.int/iris/handle/10665/328717.
- 009Wright KW, Christensen LE, Noguchi BA (1992) Results of Late Surgery for Presumed010Congenital Cataracts. American Journal of Ophthalmology 114:409–415.
- Zerr P, Ossandón JP, Shareef I, Van der Stigchel S, Kekunnaya R, Röder B (2020) Successful
 visually guided eye movements following sight restoration after congenital cataracts.
 Journal of Vision 20:3.
- Zohary E, Harari D, Ullman S, Ben-Zion I, Doron R, Attias S, Porat Y, Sklar AY, Mckyton A
 (2022) Gaze following requires early visual experience. Proc Natl Acad Sci USA
 119:e2117184119.

Active vision despite congenital blindness

1024

1019 Video 1 and Video 2. Examples of visual exploration patterns. Each subpanel shows the 1020 exploration of one participant for the complete period of image presentation. Each red dot 1021 represents one eye-tracking gaze sample (down sampled from 500 Hz to 125 Hz for better 1022 visualization) overlaid on a line-drawing sketch of the original photographic grayscale image; 1023 note that participants watched the original grayscale images.

1025 Figure 1. Eye movement kinematics during the visual exploration of an example image. (a) Examples of eye movement recordings of one participant from each group. Images were explored 1026 1027 for 4 seconds. The left panels depict the gaze traces overlaid on a line-drawing sketch of the 1028 original photographic grayscale image; note that participants watched the original grayscale 1029 images. The right panels show eve movement traces as they progress over time and space along 1030 the horizontal (dark lines) and vertical (light lines) dimension. See Extended data Fig. 1-1 and 1-2 1031 which show two other examples of eye movement recordings. (b) Distribution of the magnitude 1032 of instantaneous gaze velocity. Light lines indicate each participant's distribution and dark lines 1033 each group's average distribution. Colored circles display each participant's median value, and the yellow dots and error bars display the group's mean and s.e.m. See Extended data Fig. 1-3 for 1034 statistics. (c) Distribution of instantaneous gaze velocity (bin size = 16° /s, densities were 1035 1036 individually generated for each participant and then averaged across the participants of each 1037 group). The color scale indicates the probability of a given gaze velocity in \log_{10} scale. Yellow 1038 and white contours indicate areas that span approximately 75% and 90% of the distribution. In all 1039 figures, significant contrasts among groups are indicated with one, two or three "*" corresponding to p-values of < 0.01, < 0.001, and < 0.0001, respectively. CC – congenital cataract group; SC – 1040 1041 normally sighted controls; DC – developmental cataract controls; NC – nystagmus controls.

1043 Figure 2. Examples of visual exploration by group. The subpanels show, for different images 1044 and the four groups of participants (see Figure 1 for description) the spatial distributions of the 1045 probabilities to gaze different locations (pooled across participants and smoothed with a 2D Gaussian unit kernel), superimposed over line-drawing sketches of the original images. Warmer 1046 colors indicate higher probability to gaze a location. Yellow contours indicate areas that span the 1047 top 50%, 75% and 95% of the spatial distribution. As this distribution are constructed from all 1048 1049 gaze eye-tracking samples (each occurring every 2 ms), these maps are equivalent to the spatial 1050 distributions of dwell time. The mean of entropy and AUC values for each of the four images are 1051 indicated by the corresponding symbol (star, square, and left and right pointing triangles) in Fig. 3b,d. The last column shows the DG-II and ICF predictor maps for each image. Extended data 1052 1053 Fig. 2-1 show the grand average of the spatial distributions of the probability to gaze a certain 1054 location across all images separately for each of the four groups. In addition, the corresponding 1055 grand average DG-II and ICF predictor maps are displayed.

1056

1057 Figure 3. Spatial spread and predictability of visual exploration patterns. (a) Mean gaze 1058 entropy for each group (yellow dot with error bars, indicating the standard error of the mean) as well as for individual participants (colored dots). See Extended data Fig. 3-1 for statistics. (b) CC 1059 1060 participants gaze entropy per image compared to the gaze entropy values of the other three control 1061 groups. Colored continuous lines indicate a linear regression line for entropy values of the CC 1062 group (x-axis) and each one of the three control groups (SC: blue; DC: green; NC: orange). The 1063 top left inset depicts the corresponding Pearson's correlation values (in a red scale, upper right 1064 corner) and the corresponding p-values (in green, lower left corner). Asterisks indicate significant 1065 correlations after controlling for multiple comparisons (alpha = 0.05/6). (c) AUC values of the SC 1066 predictor map per participant and group. Dark colored dots indicate AUC values for individual 1067 participants as derived by the SC group's predictor maps to classify gaze and non-gazed location.

1068 Light colored circles from the corresponding AUC values for the control analysis in which image 1069 correspondence was shuffled. Bottom colored stars indicate that actual and control analysis values 1070 significantly differed. The control analysis values were not different from 0.5 (chance level). See Extended data Fig. 3-2 for statistics and Extended data Fig. 3-3 for the relationship between AUC 1071 1072 values and different CC participants' characteristics. (d) AUC values of the SC predictor map 1073 across time. Curves show, for each group, AUC values calculated from consecutive 500 ms data 1074 partitions. See Extended data Fig. 3-4 for statistics. (e) AUC values of the SC predictor map as a 1075 function of instantaneous gaze velocity. SC predictor maps were used to calculate gaze in CC individuals separately for ten quantiles of instantaneous gaze velocity. See Extended data Fig. 3-5 1076 for statistics. Extended data Fig. 3-6 show the relationship between gaze velocity during fixations 1077 (SC and DC groups) and CC and NC participants' 1st and 2nd instantaneous gaze velocity 1078 1079 quantiles (f) Correlations of entropy and AUC values across all images for the CC group. 1080 Different object categories are color coded. Extended data Figure 3-7 show the same correlation 1081 for SC, NC, and DC groups.

1082

1083

1084 Figure 4. Degree of explained visual exploration behavior for low- and high-level visual 1085 information and context. (a) AUC values resulting from the low-level ICF predictor maps. See 1086 Extended Data Fig. 4-1 for statistics. (b) AUC values resulting from the high-level DG-II 1087 predictor maps. See Extended Data Fig. 4-2 for statistics. (c) Ratio between ICF and DG-II AUC 1088 values. See Extended Data Fig. 4-3 for statistics. Extended data Fig. 4.4-6 show AUC values of 1089 the ICF and DG-II predictor map across time and the corresponding statistics. Extended data 1090 Figure 4-7 shows the ratio between ICG and DG-II AUC values obtained from low-pass filtered 1091 versions of the images and the AUC values obtained from the non-filtered images. See Extended 1092 data Fig. 4-8 to 4-9 for statistics.

Active vision despite congenital blindness

1094 Figure 5. Effect of stimulus repetition and object recognition performance. (a) Gaze entropy 1095 for the first vs. the second presentation of the same image (si), different images from the same 1096 object category (soc), and different images from different object categories (doc). See Extended 1097 data Fig. 5-1,2,3 for statistics. (b) Percentage correct images recognized for in each group (mean 1098 group performance in black with error bars indicating the standard error of the mean). See 1099 Extended data Fig. 5-4 for statistics (c) Recognition performance, visual acuity (logMar) and 1100 AUC values (obtained using SC predictor maps) for each CC individual. The blue shade mesh 1101 depicts the generalized logistic fit. Black lines starting at the red dots indicate the discrepancy 1102 between actual performance of a CC participant and model predictions. See Extended data Fig. 5-1103 5 for statistics Extended data Figure 5-6,7 show the relationship between Performance vs. age at 1104 testing.

individuals. (b) Visual acuity (in decimal) vs age at testing for all groups. 1107 1108 Extended data Figure 1-1. Examples of eye movement recordings of one participant from each 1109 of the four groups. 1110 Extended data Figure 1-2. Examples of eye movement recordings of one participant from each 1111 1112 of the four groups. Extended data Figure 1-3. Instantaneous gaze velocity statistical result. 1113 1114 Extended data Figure 2-1. Exploratory and feature bias. (a) Grand average, across all image 1115 and participants (per group), of the spatial distributions of the probability to gaze. (b) Grand 1116 average, across all images, of DG-II and ICF predictor maps. 1117

Extended data Table 1-1. (a) Visual acuity (in decimal) vs. age of surgery for the CC and DC

1118

1106

1119 Extended data Figure 3-1. Entropy statistical result

1120 Extended data Figure 3-2. AUC (SC predictor map) statistical result

1121 Extended data Figure 3-3. Relationship between SC predictor map AUC values in CC

1122 individuals and (a) logMAR visual acuity, (b) age at testing, (c) age at surgery, and (d) time from1123 surgery.

1124 Extended data Figure 3-4. AUC (SC predictor) per time interval statistical result

1125 Extended data Figure 3-5. AUC (SC predictor) per velocity quantile statistical result

1126 Extended data Figure 3-6. Fixational gaze velocity SC and DC groups and 1st and 2nd

- 1127 quantiles of gaze velocity in the CC and NC groups. Top panel show the grand average
- 1128 distribution, for the SC and DC groups, of the magnitude of instantaneous gaze velocity for
- 1129 samples corresponding to fixations. The lower panel show gaze instantaneous velocity first and
- 1130 second decile values for each CC and NC participant.

1146

1131 Extended data Figure 3-7. Correlation across images between entropy values and AUC

1132 values. (a) SC, (b) NC, and (c) DC groups.

1133

- 1134 Extended data Figure 4-1. AUC (ICF predictor map) statistical result
- 1135 Extended data Figure 4-2. AUC (DG-II predictor map) statistical result
- 1136 Extended data Figure 4-3. ICF/DG-II AUC ratio statistical result
- 1137 Extended data Figure 4-4. AUC values across time. Curves show, for each group, AUC values
- 1138 calculated from consecutive 500 ms data partitions. (a) ICF predictor. (B) DG-II predictor. See
- 1139 Extended data Fig. 4-5 and 4-6 for statistics.

1140 Extended data Figure 4-5. AUC (ICF predictor) per time interval statistical result

1141 **Extended data Figure 4-6**. AUC (DG-II predictor) per time interval statistical result

1142 Extended data Figure 4-7. Ratio between AUC values for saliency predictor map obtained from

1143 low-pass filtered versions of the images and the AUC values obtained from the non-filtered

1144 images, for (a) the ICF and (b) DG-II predictor maps. ICF and DG-II saliency models were run

1145 with low-pass filtered versions of the images using a 0.5, 1, and 2 visual degrees spatial frequency

cut-off. Group differences were evaluated separately per predictor map and filtered version with

1147 robust linear model contrasts. The ratio between ICF predictor map AUC values from images

1148 filtered at 0.5° and non-filtered images was higher in the CC group compared to the SC group

1149 $(t_{(38)} = -2.82, p = 0.007, \text{ see Extended data Fig. 4-8 for statistics})$ and the DC group $(t_{(38)} = -3.51, p = -3.51)$

1150 = 0.001), but not significant different from the NC group ($t_{(38)}$ = -1.06, p = 0.29). No difference

1151 between groups was found for the 1° ratio or 2° ratio AUC. The ratio between DG-II predictor

1152 map AUC values from images filtered at 0.5° and non-filtered images was higher in the CC and

1153 NC groups compared to the SC and DC group (all four *contrast*, p < 0.007, see Extended data Fig.

- 1154 4-9), but not different in the comparison between CC and NC (p = 0.79). The ratio between AUC
- 1155 values from images filtered at 1° and non-filtered images was higher in the CC compared to the

1156 DC group (p = 0.005). No other group contrast was significant. No group difference was found 1157 for the DG-II 2°. In summary, compared to SC and DC participants for CC and NC participants 1158 gazed- and non-gazed locations were to a larger degree predicted by the low spatial spectral

1159 content of the images.

1160 Extended data Figure 4-8. AUC (ICF predictor map low pass 0.5 filtered) statistical result

1161 Extended data Figure 4-9. AUC (DG-II predictor map low pass 0.5 filtered) statistical result
1162

1163 Extended data Figure 5-1. Entropy values for the first vs. second image of a pair of identical
1164 images statistical result

1165 Extended data Figure 5-2. Entropy values for the first vs. second image of a pair of images from
1166 same category statistical result

1167 Extended data Figure 5-3. Entropy values for the first vs. second image of a pair of images from

1168 different category statistical result

1169 Extended data Fig. 5-4. Performance for each group statistical result

1170 Extended data Fig. 5-5. CC participants' performance statistical result.

1171 Extended data Fig. 5-6. Performance vs. age at testing. Age at testing was not correlated with

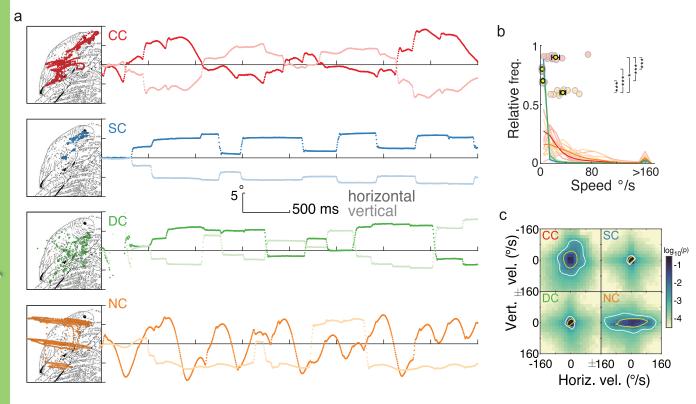
1172 performance across all participants (r = 0.06, p = .69) nor when tested only for the CC group (r = .69)

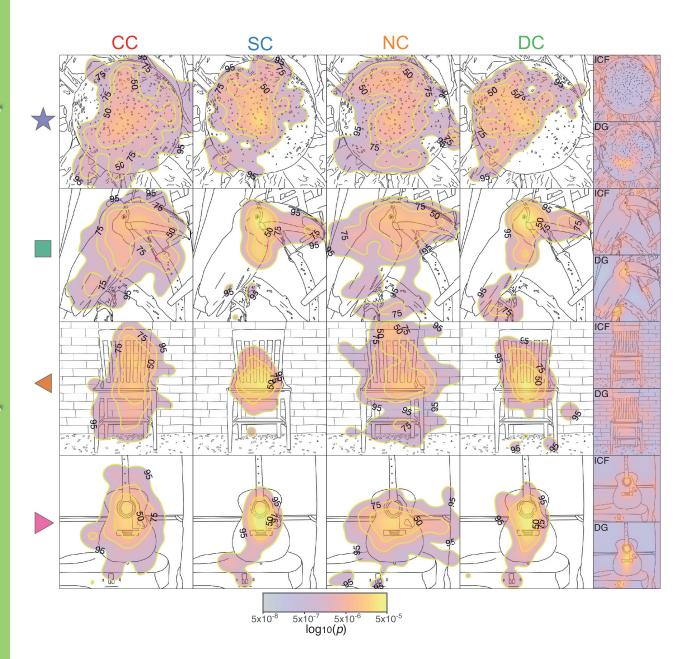
1173 .1, p = .78). For CC participants, a logistic regression model analysis showed no association

1174 between object recognition performance and age at testing (p = 0.17, see Extended data Fig. 5-7).

1175 **Extended data Fig. 5-7.** CC participants' performance and age statistical result.

eNeuro Accepted Manuscript





eNeuro Accepted Manuscript

